

# A numerical study of the interannual variability of the Adriatic Sea (2000–2002)

Paolo Oddo\*, Nadia Pinardi, Marco Zavatarelli

*Università degli Studi di Bologna, Corso di Scienze Ambientali, Laboratorio di Simulazioni Numeriche del Clima e degli Ecosistemi Marini,  
Via S.Alberto 163 Ravenna Italy*

Available online 27 October 2005

## Abstract

A free-surface, three-dimensional finite-difference numerical model based on the Princeton Ocean Model (POM) has been implemented in order to simulate the interannual variability of the Adriatic Sea circulation. The implementation makes use of an interactive surface momentum and heat flux computation that utilizes the European Centre for Medium-Range Weather Forecasts (ECMWF) 6-h analyses and the model predicted sea surface temperatures. The model is also nested at its open boundary with a coarse-resolution Mediterranean general circulation model, utilizing the same surface forcing functions. The simulation and analysis period spans 3 years (1 Jan 2000 to 31 Dec 2002) coinciding with the “Mucilage in the Adriatic and the Tyrrhenian” (MAT) Project monitoring activities. Model results for the simulated years show a strong interannual variability of the basin averaged properties and circulation patterns, linked to the atmospheric forcing variability and the Po river runoff. In particular, the years 2000 and 2002 are characterized by a weak surface cooling (with respect to the climatological value) and well-marked spring and autumn river runoff maxima. Conversely, 2001 is characterized by stronger wind and heat (autumn cooling) forcings but no river runoff autumn peak, even though the total amount of water inflow during winter and spring is sustained. The circulation is characterized by similar patterns in 2000 and 2002 but very different structures in 2001. During the latter, deep water is not formed in the northern Adriatic. A comparison with the observed data shows that the major model deficiencies are connected to the low salinity of the waters, probably connected to the missed inflow of salty Ionian waters of Aegean origin and to the numerical overestimation of the vertical mixing processes.

© 2005 Elsevier B.V. All rights reserved.

*Keywords:* Adriatic Sea circulation; Numerical modeling; Interannual variability; Air–sea interactions

## 1. Introduction

The semi-enclosed Adriatic Sea extends in a NNW–SSE direction for about 770 km and has a mean width of about 160 km. The basin is conventionally divided on the basis of its bottom morphology into three sub-basins: the northern, the middle and the southern (Fig. 1). The northern basin with an average depth of 35 m

has truly coastal characteristics. The middle Adriatic has depths increasing from north to south and is marked by two bottom depressions reaching about 250 m in depth. The transition from the middle to the southern sub-basin occurs with a sharp bathymetry gradient from about 200 m to depths exceeding 1000 m. Exchanges with the Ionian Sea occur through the Otranto Channel, the morphology of which is marked by a sill of about 900 m in depth.

The surrounding orography, basin morphology, atmospheric forcing, river runoff, and exchanges through the Otranto Channel constrain the Adriatic’s general

\* Corresponding author. Tel.: +39 544 600325; fax: +39 544 600323.

*E-mail address:* [p.oddo@ambra.unibo.it](mailto:p.oddo@ambra.unibo.it) (P. Oddo).

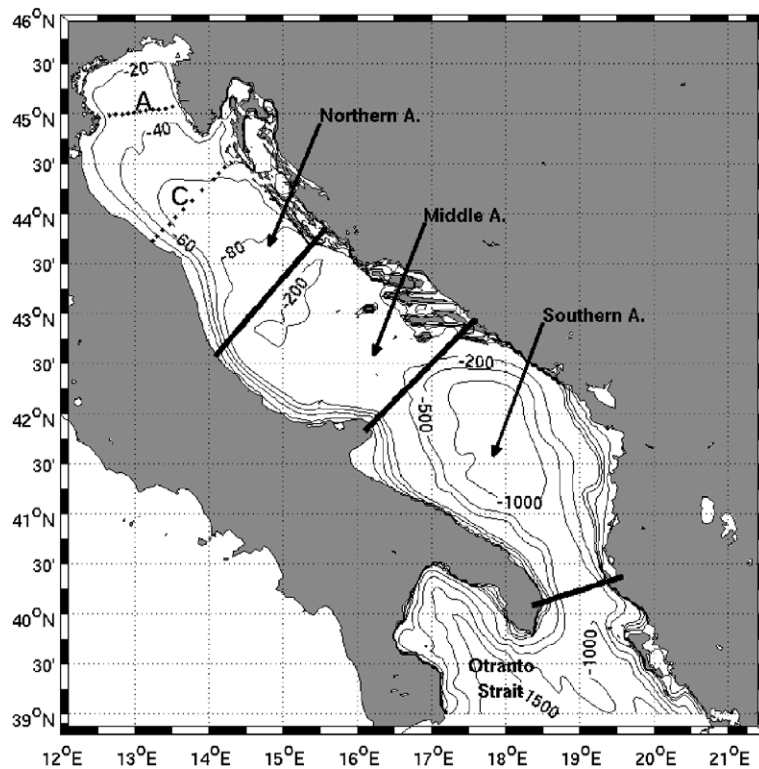


Fig. 1. Bathymetry of the Adriatic Sea. The sub-basins studied in the paper are defined. The location of the MAT transects are also indicated (letters A and C in the northern sub-basin). Depths are given in meters.

circulation. The two major wind regimes are the Bora (NNE) and the Scirocco (SE). The Bora blows over the Adriatic in intense episodic bursts. Its field over the Adriatic Sea is strongly influenced by the orography of the eastern Adriatic land margins (Vilibic, 2003), giving rise to a strong spatial variability (Orlic et al., 1994). The Scirocco is connected with the passage of low-pressure systems over the basin, causing the relative increase in sea level in this region due to the inverse barometer effect and to the direct sea level set-up by the wind. This effect is particularly strong in the northern Adriatic (Orlic et al., 1992; Lascaratos and Gacic, 1990).

The river runoff is a significant component of the basin hydrological cycle and is responsible for the basin net freshwater gain (Raicich, 1994, 1996), implying an average estuarine thermohaline circulation. The freshwater discharge is particularly concentrated in the northern sub-basin, where the river Po constitutes the main freshwater source. However, in the southern basin, the ensemble of Albanian and Croatian rivers provides a significant freshwater input (Raicich, 1994).

The annual heat budget is negative at the climatological scale ( $-17, -22 \text{ W m}^{-2}$ , Artegiani et al., 1997a), but it is known to experience significant year-to-year variations sometimes being positive (Maggiore

et al., 1998; Cardin and Gacic, 2003; Chiggiato et al., 2005—this issue). The climatological negative heat budget implies the establishment of an antiestuarine thermohaline circulation, contrasting the effects of the freshwater flux. The basin is a well-known site of dense water formation related to the winter surface heat losses, as well as to the ingression into the basin of Levantine Intermediate Water. Dense water formation processes occur in the northern shelf (Malanotte Rizzoli, 1991) and in the open Southern Adriatic (Ovchinnikov et al., 1997; Artegiani et al., 1989; Manca et al., 2002). The formation processes are known to be highly variable at the interannual time scales (Manca et al., 2002). The climatological circulation pattern is composed of well-known current and gyre structures (Artegiani et al., 1997b; Poulain, 2001; Zavatarelli et al., 2002; Zavatarelli and Pinardi, 2003), such as the three cyclonic gyres located in the southern, central and northern sub-basins, named respectively by Artegiani et al. (1997b) Southern (SAD), Middle (MAd) and Northern (NAd) Adriatic gyres. The three gyres are interconnected (with seasonally varying characteristics) by two coastal currents, one flowing southward along the whole western coast from the Po delta to the Otranto Strait (Western Adriatic Coastal Current or WACC), the other flowing

northward from the Otranto Strait along the eastern coast and reaching the central Adriatic sub-basin (Eastern Southern Adriatic Current or ESAC). However, the interannual variability of these circulation structures is still poorly known and understood.

This work starts to explore the Adriatic Sea circulation interannual variability connected to atmospheric forcing by means of numerical simulations of the general circulation. We concentrated on the period 2000–2002, during which the MAT project extensively monitored the northern and middle Adriatic Sea. The circulation is simulated by a three-dimensional model already used by [Zavatarelli and Pinardi \(2003\)](#) for climatological simulations of Adriatic Sea circulation. In order to reproduce the interannual variability, the model has been forced with atmospheric data obtained from the European Centre for Medium Range Weather Forecasts (ECMWF) analyses, daily Po discharges and lateral boundary conditions from a Mediterranean Sea general circulation model ([Pinardi et al., 2003](#)). To our knowledge this is the first time that such an interannual variability simulation has been carried out and compared with data.

Section 2 gives a general description of the model implementation. Section 3 describes the model results and discusses the comparison with observed data. Conclusions are offered in the last section.

## 2. Model design

The numerical simulation of the Adriatic Sea general circulation has been carried out using the Adriatic Sea Regional Model (AREG) based on the Princeton Ocean Model, POM ([Blumberg and Mellor, 1987](#)) as implemented by [Zavatarelli and Pinardi \(2003\)](#). POM is a free-surface, three-dimensional finite-difference numerical model based on the primitive equations with Boussinesq and hydrostatic approximations. All the equations are written in rectangular coordinates and contain spatially and temporally varying horizontal eddy viscosity and diffusion coefficients. The model solves the following equations for the ocean velocity  $U=(u,v,w)$ , potential temperature  $\theta$  and salinity  $S$ :

$$\nabla \cdot U = 0 \quad (1)$$

$$\begin{aligned} \frac{\partial(u,v)}{\partial t} + U \cdot \nabla(u,v) + f(-v,u) \\ = -\frac{1}{\rho_0} \left( \frac{\partial p}{\partial x}, \frac{\partial p}{\partial y} \right) + \nabla_h \cdot [A_M \nabla(u,v)] \\ + \frac{\partial}{\partial z} \left[ K_M \frac{\partial(u,v)}{\partial z} \right] \end{aligned} \quad (2)$$

$$\frac{\partial \theta}{\partial t} + U \nabla \theta = \nabla_h \cdot [A_M \nabla_h \theta] + \frac{\partial}{\partial z} \left[ K_H \frac{\partial \theta}{\partial z} \right] + \frac{1}{\rho_0 C_P} \frac{\partial I}{\partial z} \quad (3)$$

$$\frac{\partial S}{\partial t} + U \cdot \nabla S = \nabla_h \cdot [A_M \nabla_h S] + \frac{\partial}{\partial z} \left[ K_H \frac{\partial S}{\partial z} \right]. \quad (4)$$

The eddy viscosity coefficient  $A_M$  is provided by the [Smagorinsky \(1993\)](#) parameterization implemented into POM according to [Mellor and Blumberg \(1985\)](#). The vertical mixing coefficients for momentum  $K_M$  and tracers  $K_H$  are calculated using the [Mellor and Yamada \(1982\)](#) turbulence closure scheme. The last term in Eq. (3) is the parameterization of the heat penetration in the water column ([Pinardi et al., 2003](#)):  $\rho_0$  is a reference density,  $C_P$  is the water specific heat and  $I(z)$  is defined according to:

$$I(z) = Tr Q_s e^{-\lambda z}$$

where  $Q_s$  is the short-wave radiation flux and  $Tr$  and  $\lambda$  are the [Jerlov \(1976\)](#) transmission and absorption coefficients for which we adopted those corresponding to the “clear” water type.

Finally, the hydrostatic approximation yields,

$$\frac{\partial p}{\partial z} = -\rho(S, \theta, p)g \quad (5)$$

where  $\rho$  is the density calculated by an adaptation of the UNESCO equation of state devised by [Mellor \(1991\)](#).

AREG uses the [Smolarkiewicz \(1984\)](#) iterative positive definite advection scheme for tracers as implemented into POM by [Sannino et al. \(2002\)](#).

### 2.1. Surface and lateral boundary conditions

In order to parameterize the air–sea interaction processes, the wind stress, the heat fluxes and evaporation rate are computed by means of interactive bulk formulae making use of atmospheric data and the model predicted sea surface temperature. The resulting surface boundary conditions for momentum and tracers are:

$$\rho_0 K_M \frac{\partial(u,v)}{\partial z} \Big|_{z=\eta} = (\tau_{wx}, \tau_{wy}) \quad (6)$$

$$\begin{aligned} \rho_0 K_M \frac{\partial \theta}{\partial z} \Big|_{z=\eta} = \frac{1}{C_P} \left[ (1 - Tr) Q_s(C) \right. \\ \left. - Q_B(T_a, \theta_{z=\eta}, C, rh) \right. \\ \left. - Q_e(T_a, \theta_{z=\eta}, rh, |\bar{v}_w|) \right. \\ \left. - Q_h(T_a, \theta_{z=\eta}, |\bar{v}_w|) \right] \end{aligned} \quad (7)$$

$$K_H \frac{\partial S}{\partial z} \Big|_{z=\eta} = S_{z=\eta} (E - P - R) \quad (8)$$

where  $\eta$  is the free surface elevation. The wind stress ( $\tau_{wx}, \tau_{wy}$ ) computation uses a drag coefficient computed according to [Hellerman and Rosenstein \(1983\)](#).

The surface boundary condition for temperature (Eq. (7)) involves the balance between surface solar radiation ( $Q_S$ ), net long-wave radiation ( $Q_B$ ), the latent and sensible heat fluxes ( $Q_e, Q_h$ ). Solar radiation is dependent on cloud cover ( $C$ ) and is computed by means of an astronomical formula ([Reed, 1975, 1977](#)). The net long-wave radiation flux ([May, 1986](#)) is a function of air temperature ( $T_a$ ), sea-surface temperature ( $\theta_{z=\eta}$ ), cloud cover  $C$  and relative humidity (rh). Sensible heat flux and latent heat flux are computed by classical bulk formulae parameterized according to [Kondo \(1975\)](#). Details on the bulk formulae used can be found in [Maggiore et al. \(1998\)](#) and [Castellari et al. \(1998\)](#).

Surface salinity flux in Eq. (8) is given by the water balance  $E - P - R$ , where  $E$  is the evaporation (derived from the latent heat flux),  $P$  the precipitation and  $R$  the river-runoff multiplied by the model predicted surface salinity  $S_{z=\eta}$ .  $R$  is a non-zero value only at the “estuary” grid points.

POM traditionally uses only the kinematics vertical velocity boundary conditions, i.e.,

$$w|_{z=\eta} = \left( \frac{\partial}{\partial t} + u \frac{\partial}{\partial x} + v \frac{\partial}{\partial y} \right) \eta.$$

This means that in our model version the surface water flux does not produce volume changes but only salt changes.

Lateral open boundary conditions are defined through a simple off-line, one-way nesting technique. AREG is nested with the general circulation model of the Mediterranean Sea (OGCM) developed by [Demirov and Pinardi \(2002\)](#). In order to ensure that the volume transport across the open boundary of AREG matches the volume transport across the corresponding section of the OGCM, the total velocity component normal to the boundary was corrected on the basis of the differences between the volume transport computed on the AREG and on the OGCM grid ([Pinardi et al., 2003; Zavatarelli and Pinardi, 2003](#)). The vertically integrated velocity component normal to the boundary in AREG is defined as

$$V_{\text{AREG}} = \left[ \frac{H_{\text{OGCM}}}{(\eta + H_{\text{AREG}})} \right] V_{\text{OGCM}} \quad (9)$$

where  $H_{\text{OGCM}}$  and  $H_{\text{AREG}}$  are the OGCM and AREG bottom depths along the open boundary,  $\eta$  is the AREG free surface elevation and  $V_{\text{OGCM}}$  is the OGCM vertically integrated velocity. Temperature and salinity on the outflow are locally resolved with an upwind scheme, while, if there is an inflow, they are prescribed from the OGCM. Differently from [Zavatarelli and Pinardi \(2003\)](#), in the AREG interior, immediately adjacent to the boundary, a nudging term was added (following [Marchesiello et al., 2001](#)) to the right-hand side (r.h.s.) of the prognostic equations for tracers, as follows:

$$\frac{\partial \gamma}{\partial t} = \text{r.h.s.} - \frac{1}{\Gamma} (\gamma - \gamma^{\text{OGCM}})$$

where  $\gamma$  can indicate temperature or salinity.  $\Gamma$  varies smoothly from few days at the boundary to (almost) infinity at a distance from the open boundary of approximately 50 km.

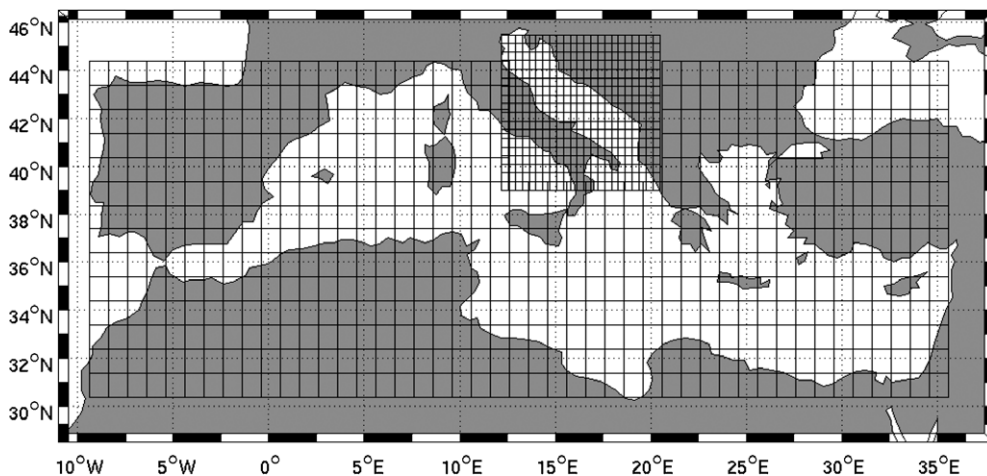


Fig. 2. AREG and OGCM models domains. The horizontal resolution of both grids is undersampled.

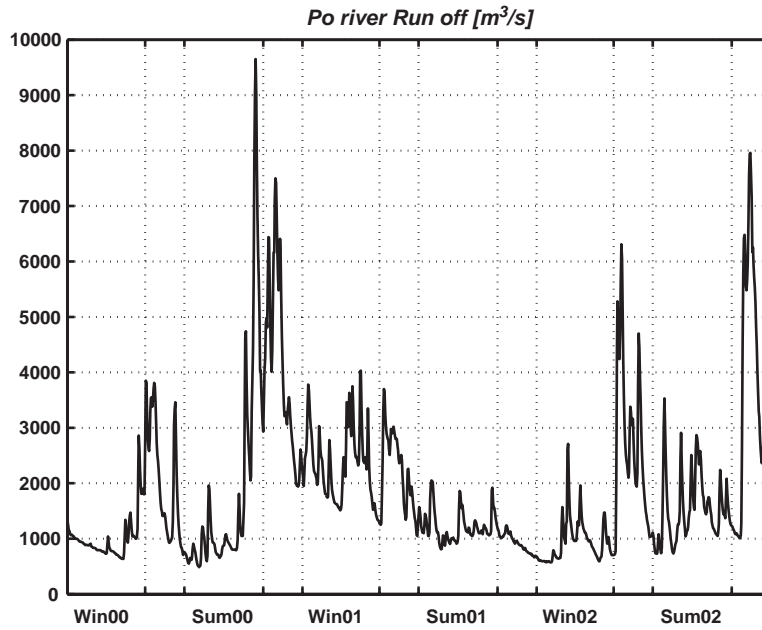


Fig. 3. Time series of the Po river runoff ( $\text{m}^3/\text{s}$ ) for the model simulation period (2000–2002).

2.2. Simulation experiments design

AREG has been implemented on a regular horizontal grid with approximately 5 km resolution (the extension of the model domain is reported in Fig. 2) and 21 vertical sigma layers. The bathymetry has been

obtained from U.S. Navy data (horizontal resolution:  $1/60^\circ$ ), the minimum depth has been set to 10 m. The model has only one open boundary located south of the Otranto Channel where it is nested with the OGCM (Fig. 2). Integration started at 00:00 on January 1. As initial condition, the fields from the climatological

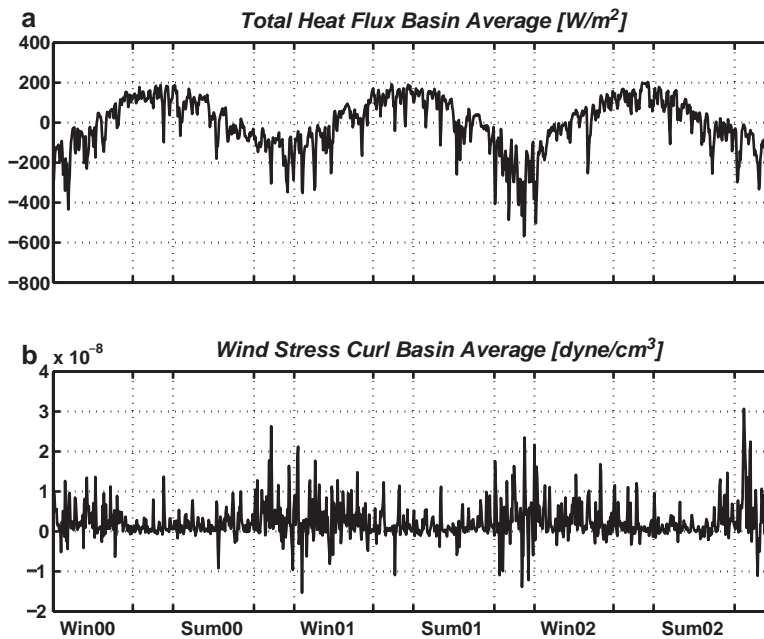


Fig. 4. Temporal evolution of the basin-averaged (a) total heat fluxes ( $\text{W m}^{-2}$ ), (b) wind stress curl ( $\text{dyn cm}^{-3}$ ) for the model simulation period (2000–2002).

Table 1

Heat flux ( $\text{W}/\text{m}^2$ ) and its differences (%) with the climatology computed by Maggiore et al. (1998)

	Clim	2000	2000 (%)	2001	2001 (%)	2002	2002 (%)
Winter	-75	-55	-26	-40	-46	-22	-70
Spring	177	126	-28	124	-29	131	-25
Summer	52	28	-46	38	-26	21	-59
Autumn	-225	-132	-41	-242	7	-127	-43
Annual	-17	-9	-47	-18	5	1	-105

The difference is defined as:  $[(\text{model} - \text{climatology}) / \text{climatology}] * 100$ . Seasonal and annual means are reported.

simulation of the Adriatic Sea circulation (Zavatarelli and Pinardi, 2003) were used. The atmospheric data for the computation of the surface forcing were obtained from the 6-h,  $0.5^\circ$  horizontal-resolution ECMWF surface analyses. The atmospheric fields used are air temperature, dew point temperature, wind velocity at 10 m above sea level, mean sea level pressure and cloud cover. Precipitation data were obtained by interpolation of the  $0.5^\circ$  resolution Legates and Wilmott (1990) climatological global, monthly averaged precipitation data set into the model grid. The river runoff data for the major Adriatic Sea rivers, Po excluded, were obtained from the Raicich (1994) monthly climatology. The major Adriatic rivers were considered as point sources, while non-point contributions were defined as an evenly distributed source along the pertinent portion of coastline. Po

river runoff values are not climatological but we used the daily averages for the period 1999–2002 measured by the Po River Authority at the closing point of the drainage basin. The Po runoff is distributed over 6 grid points approximately representing the partitioning of the freshwater discharge through the mouths of the delta (Provini et al., 1992). The 2000–2002 time series of the Po river runoff is shown in Fig. 3. A large interannual variability is evident, marked mainly by three main events: a large maximum in autumn 2000, a sustained runoff for a large part of winter and spring 2001 and the absence of runoff maximum in autumn 2001.

### 3. Model simulations

In this section, we describe the model simulation results for the period from January 2000 to December 2002. Results for year 1999 are not shown as the relative simulation is considered to represent the model spin-up period.

#### 3.1. Diagnosed surface fluxes

Time series of the basin-averaged daily mean heat flux and wind stress curl are shown in Fig. 4. The heat flux time series shows similar summer maximum values (about  $200 \text{ W m}^{-2}$ ) and large differences in the minima (ranging from  $-380 \text{ W m}^{-2}$  in autumn

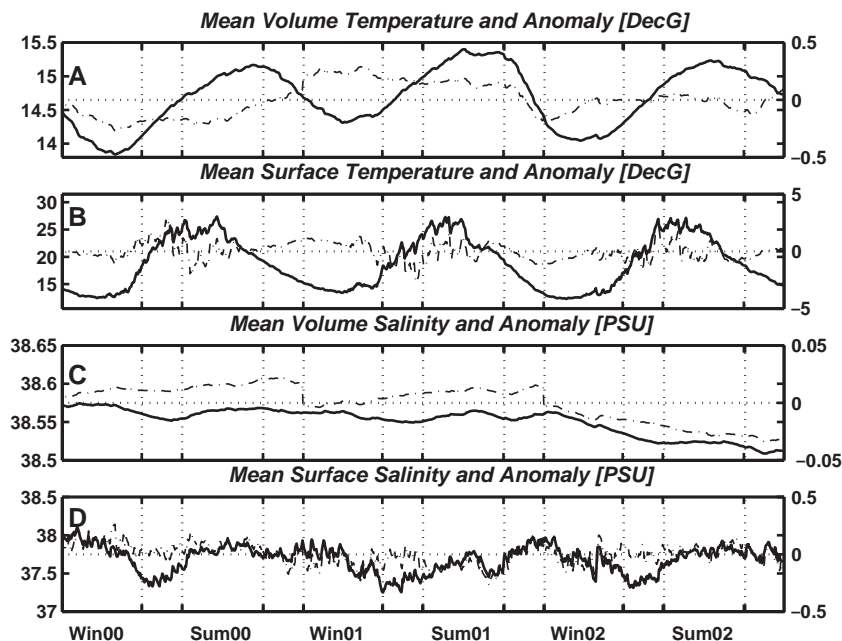


Fig. 5. Temporal evolution of the basin and surface averaged scalar proprieties (solid lines) and the corresponding anomaly (dash lines). (A) Mean volume temperature ( $^\circ\text{C}$ ). (B) Mean surface temperature ( $^\circ\text{C}$ ). (C) Mean volume salinity (psu). (D) Mean surface salinity (psu).

2000 and 2002 to  $-600 \text{ W m}^{-2}$  in 2001). The seasonally averaged heat fluxes are computed according to the season definition proposed by Artegiani et al. (1997a): Winter; January to April, Spring; May and June, Summer; July to October, Autumn; November and December, and are reported in Table 1 along with the annual average and the anomalies (percentage values) from the climatology computed by Maggiore et al. (1998). Previous computation of the climatological annual surface heat budget yielded values ranging between  $-17$  and  $-22 \text{ W m}^{-2}$  (Artegiani et al., 1997a; Maggiore et al., 1998; Cardin and Gacic, 2003). The annual average for year 2002 is instead weakly positive while the climatological value is met only in 2001. In general, the spring–summer heat gain does not change significantly from year to year. On

the contrary, the autumn and winter cooling exhibits a strong interannual variability that is mainly due to the latent heat flux (not shown) component of the surface heat balance in Eq. (7).

The time series of the basin-averaged wind stress curl (Fig. 4) is predominantly positive, therefore implying a net cyclonic vorticity input into the basin with maxima in winter. The heat flux and the wind stress curl time series reveal a strong seasonal cycle, but the wind stress curl variability is clearly dominated by shorter time scale events determining the frequent change of the sign of the basin averaged wind stress curl. We know in fact that the wind stress curl spatial distribution is characterized by positive and negative lobes, due to the multiple jet structure of Bora winds (Orlic et al., 1994). These short temporal and spatial scales are the

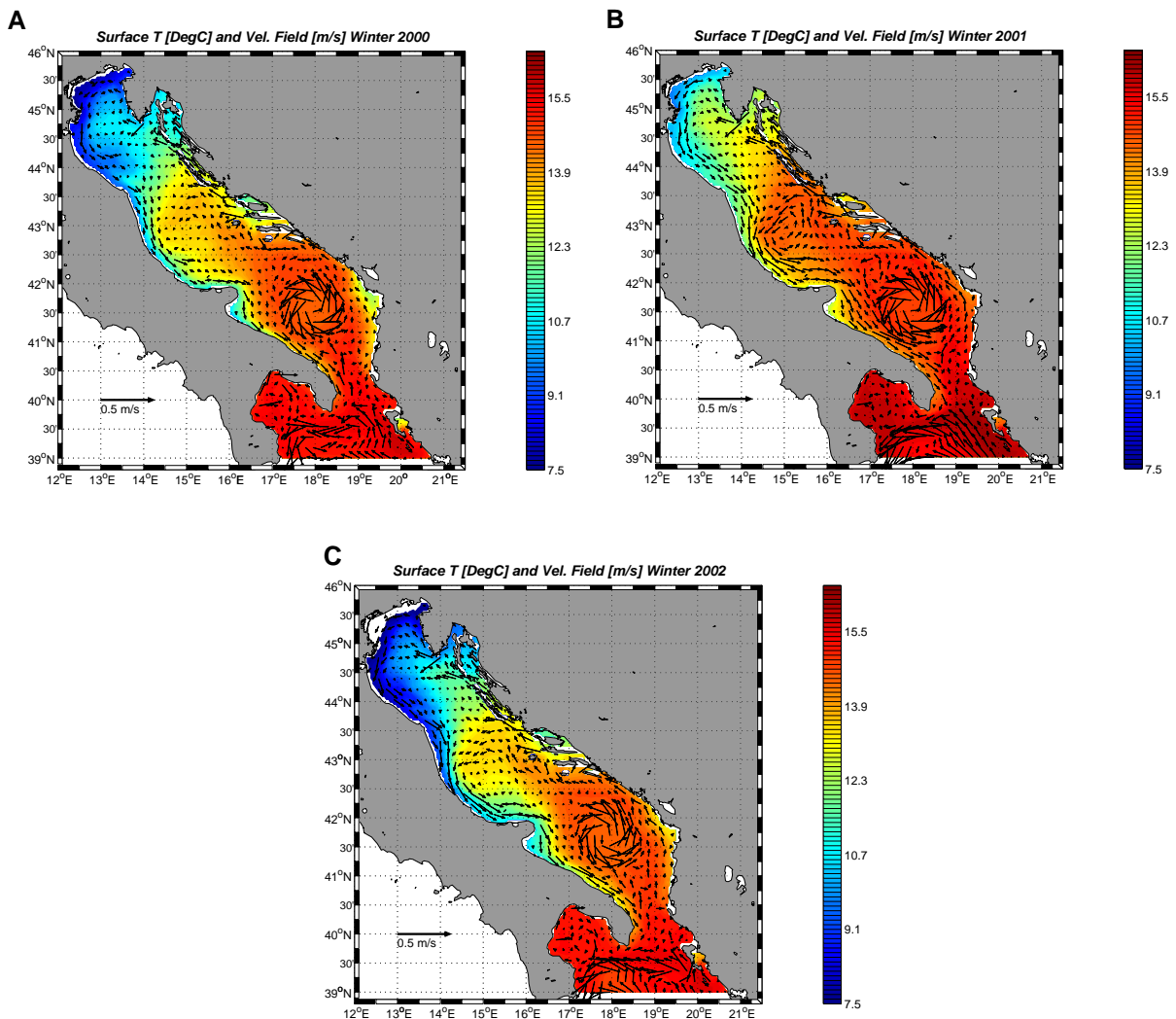


Fig. 6. Near-surface (2 m depth) temperature ( $^{\circ}\text{C}$ ) and velocity (m/s) fields for (A) winter 2000; (B) winter 2001; (C) winter 2002.

main reason for the large interannual variability of Adriatic Sea circulation.

### 3.2. The structure of the circulation in the different years

In this section, we analyze the model simulation and describe the interannual variability of Adriatic Sea circulation beginning with the analysis of the volume-integrated scalar properties and ending with the comparison between model results and observations.

The basin averaged temperature and the corresponding mean volume anomaly time series are shown in Fig. 5A and indicate a large interannual variability characterized by a maximum temperature value (15.50 °C) occurring in late summer 2001 and a minimum of about 13.80 °C in winter 2000. The former is probably

a consequence of the mild autumn–winter 2000–2001 (confirmed also by the anomaly maximum occurring during winter 2001) and, similarly, the latter is influenced by the marked heat loss occurring during the winter 2000 (Fig. 4 and Table 1). The time series of the surface-averaged temperature and its anomaly (Fig. 5B) show the same characteristics but with a less evident interannual signal during winter.

The basin-averaged salinity (Fig. 5C) does not show the marked interannual variability affecting the temperature field, remaining approximately constant at 38.57 psu throughout almost the entire simulation. The only remarkable deviation can be noted for 2002, during which the basin undergoes a freshening of about 0.04 psu. Analysis of the salt flux through the model open boundary (not shown) seems to indicate that the freshening is due to a reduced salt flux into the basin rather

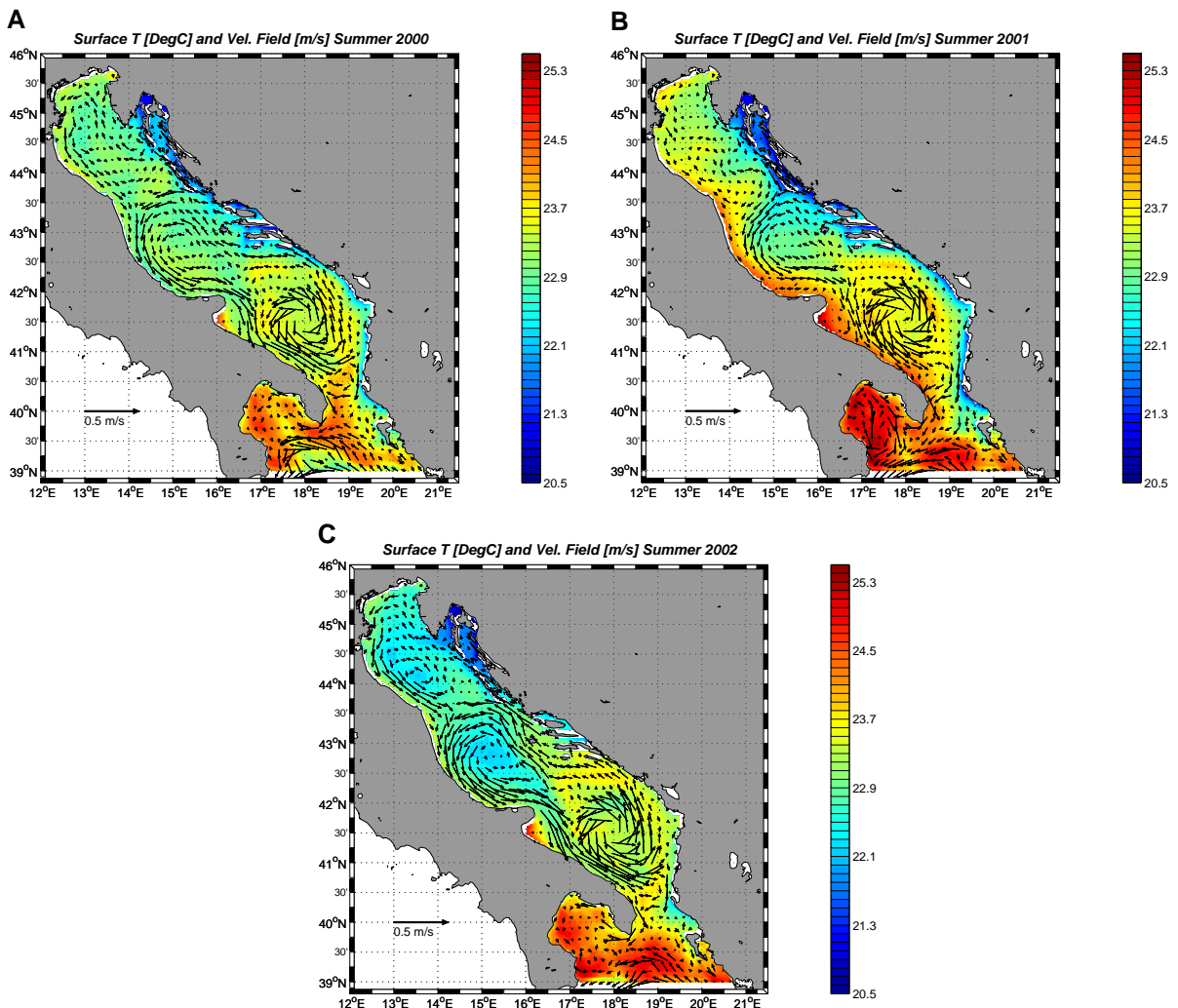


Fig. 7. Near-surface (2 m depth) temperature (°C) and velocity (m/s) fields for (A) summer 2000; (B) summer 2001; (C) summer 2002.

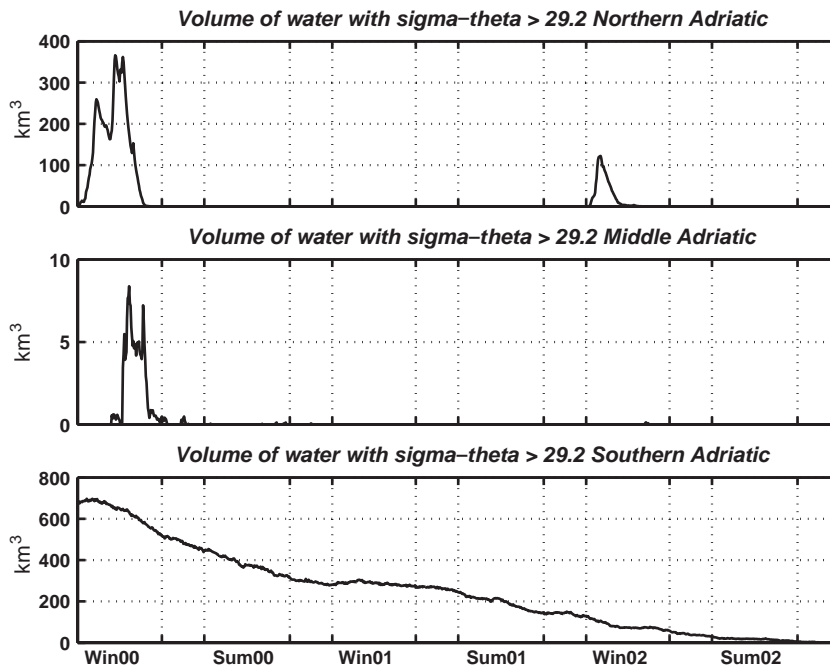


Fig. 8. Temporal evolution of the total amount of waters having  $\sigma\text{-}\theta > 29.2 \text{ kg m}^{-3}$  in the three sub-basins ( $\text{m}^3$ ).

than to a variation in the surface salt flux. In fact the time series of the surface averaged salinity (Fig. 5D) suggests an annual cycle for 2002 similar to that of previous years.

In Figs. 6 and 7 we show the winter and summer temperature and velocity near surface (2 m depth) fields. A significant difference can be noted between 2001 (Fig 6B) and both 2000 (Fig. 6A) and 2002 (Fig. 6C). The 2001 winter fields are characterized by a more energetic circulation pattern, with relatively high surface temperatures and a large and well-defined MAD gyre. The larger kinetic energy of the circulation is evident in the stronger WACC and more intense MAD and SAd gyres. The reason for this increased strength of the circulation structures can be traced back to the relatively concurrent action of mild winter heat fluxes (Table 1), high Po runoff during winter–spring and strong wind stress curl over the basin (Fig. 4b). It is in fact known that large heat losses and thus cooler waters in the northern and western coastal areas contribute to a weaker WACC (Zavatarelli et al., 2002); conversely, the strong Po runoff and the large wind stress curl would enhance it. Under large positive wind stress curl conditions, the MAD gyre is stronger as well as the SAd gyre and the ESAC.

The cooler surface temperatures in the winter of 2000 and 2002 (Fig. 6A, C) are due to large heat losses in the winter of 2000 and autumn of 2001; therefore,

the two similar surface temperature fields arise from different processes and forcings.

The three summers (Fig. 7A–C) are characterized by well-defined MAD and SAd gyres. The simulated cross-shelf extension of the WACC is larger than in the winter, in agreement with observations (Poulain, 2001). Differently from the winter fields (Fig. 6), the north-western shelves are characterized by warm temperatures on the westward side of the WACC due to downwelling motion. During winter, the WACC transports cool waters formed in the northern Adriatic and the temperatures on the westward side of the WACC are at a minimum. During summer, coastal heating prevails and allows the downwelling regime to store heat.

Interesting differences in the circulation between the three summers are the position and intensity of the NAD gyre and the strong interannual variability of the circulation along the Istrian coast. The NAD gyre is evident

Table 2  
Presence/Absence of dense waters ( $\sigma_\theta > 29.20 \text{ kg m}^3$ ) in the MAT data set used in this study

	2000	2001	2002
Winter	Presence	Absence	Presence
Spring	Presence	Absence	Presence
Summer	Absence	Absence	Absence
Autumn	Absence	Absence	Absence

in summer 2000 (Fig. 7A) and 2002 (Fig. 7C), although it is located farther to the south in 2002. On the contrary, in summer 2001 (Fig. 7B), the NAd gyre almost disappears. Concurrent with the strong weakening of the gyre is the reversal of the coastal circulation along the Istrian peninsula. The appearance of a southward current in this region, named by Supic et al. (2000) the “Istrian Coastal Countercurrent, ICC”, has been already simulated at the climatological scale by Zavatarelli and Pinardi (2003). However, the appearance of the ICC only in 2001 seems to confirm the interannual nature of such circulation pattern as originally proposed by Supic et al. (2000). A small and weak ICC can be detected also in the summer of 2000 in the northernmost part of the Istrian peninsula. However, during 2001, the overall cyclonic circulation of the northern Adriatic is the weakest of the 3 years and the ICC develops more strongly. Our results show that it is very difficult to predict the changes in the circulation directly from the atmospheric and fresh water forcing variability since

their concomitant effect is largely nonlinear in the Adriatic basin.

The variability of the dense water formation processes have been diagnosed from the model results by assessing the volume of water with  $\sigma_\theta > 29.20 \text{ kg m}^{-3}$  (in agreement with Artegiani et al., 1997b) for the three sub-basins. The daily averaged time series of water volumes are shown in Fig. 8. It can be noted that the variability patterns in the three sub-basins have different temporal evolution. The time series of the northern sub-basin is characterized by the absence of dense waters in 2001. This confirms the different characteristics of this year with respect to 2000 and 2002. This absence is probably the consequence of the reduced cooling (Fig. 4) and strong river runoff (Fig. 3) occurred in autumn–winter 2000–2001. The middle Adriatic maximum value (Fig. 8) is reached later than the corresponding maximum in the northern area. Thus, we can conclude, in agreement with Artegiani et al. (1997b), that a portion of northern Adriatic dense water

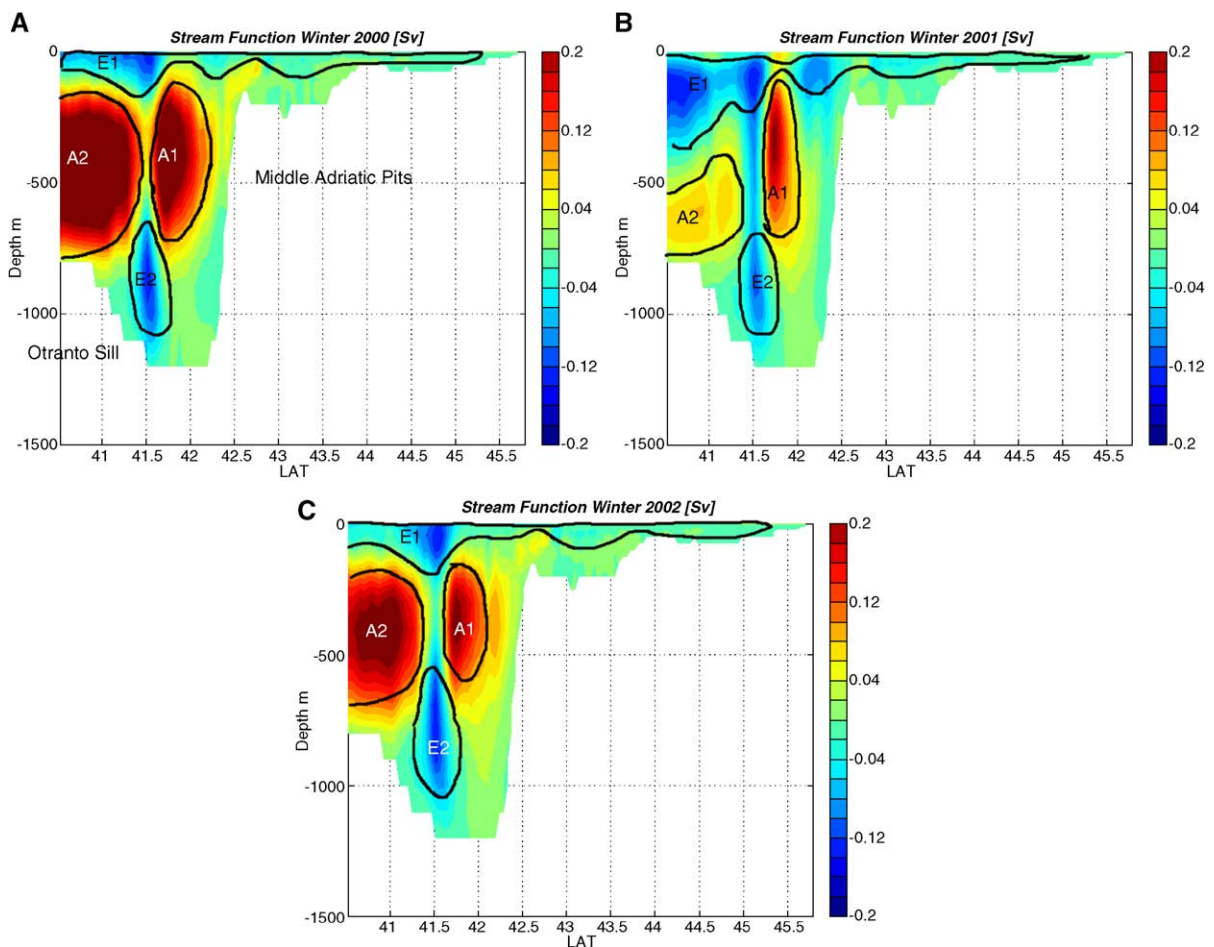


Fig. 9. Meridional transport stream function (Sv) winter mean for (A) year 2000; (B) year 2001; (C) year 2002.

**Table 3**  
 Dates of the MAT samplings in the 3 years of the project (columns) sorted according to the seasons definition of *Artegiani et al. (1997a,b)* (rows)

	2000	2001	2002
Winter	5 Jan		14 Jan
	21 Feb	6 Feb	20 Mar
	21 Mar	20 Feb	
	17 Apr	15 Mar	18 Apr
Spring			7 May
	1 Jun	29 May	4 Jun
	20 Jun	26 Jun	25 Jun
Summer	6 Jul		
	22 Jul	26 Jul	
	10 Aug	21 Aug	
	24 Aug	26 Sep	
	24 Oct	26 Oct	31 Jul
Autumn	5 Dec		
	14 Dec	22 Nov	

is advected southward toward the middle Adriatic depression. This advective process is not observed in 2002, probably because of the limited amount northern Adriatic winter dense water formed (Fig. 8). The volume of the Southern Adriatic dense water is maximum in winter 2000 and progressively decreases in 2001 and 2002.

In order to validate the model’s skill in reproducing the dense water formation process variability, we computed the sigma–theta seasonal means along transects A and C (locations shown in Fig. 1) for the MAT observations. In Table 2, the presence/absence of waters with density values greater than the threshold value ( $29.20 \text{ kg m}^{-3}$ ) are reported. We must note that dense waters are present only during the winter and spring of 2000 and 2002 in partial agreement with the model results shown in Fig. 8. We have to point out that computing, from model results, the amount of deep waters on the same sections of the MAT observations we could not find the water masses. This is probably due to the general underestimation of the model salinity as further discussed in Section 3.3. The amount of dense waters formed by the model is thus low than observed in the MAT data set. A likely consequence is the absence of the residual dense water in spring, in contrast with the MAT data set. Thus, the model solution is only in a qualitative agreement with the observations along the sections in terms of overall temporal variability.

In order to have a synthetic index of the Adriatic Sea thermohaline circulation variability, we computed the meridional transport streamfunction,  $\Psi$ ,

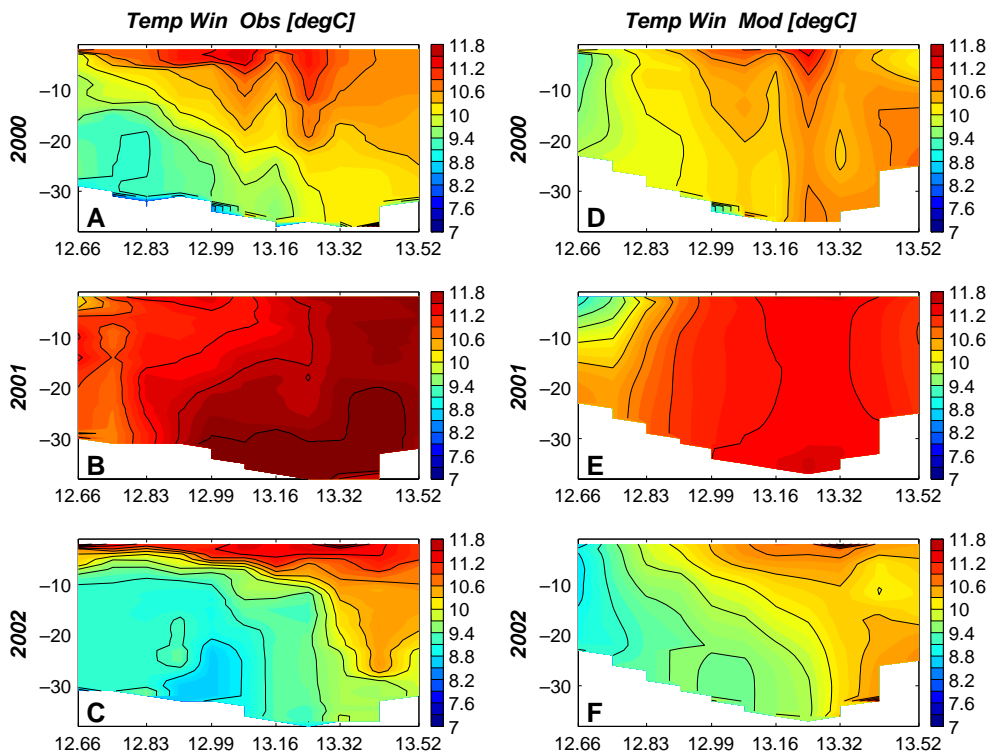


**Fig. 10.** Vertical temperature distributions ( $^{\circ}\text{C}$ ) along the transect A for the simulated winters. (A–C) 2000, 2001 and 2002 winters means from observations. (D–F) 2000, 2001 and 2002 winters means from model results. The position of the transect is reported in Fig. 1.

by integrating the total north–south transport across lines of constant longitude (Peixoto and Oort, 1992):

$$\Psi(z) = + \int_{x_0}^{x_1} \int_H^z v \, dx dz.$$

With  $H < z < \eta$ . The velocity field is now tangent to the isopleths of  $\Psi$  and this is indicative of the vertical circulation in the basin. The negative values correspond to an estuarine cell turning cyclonically around the negative  $\Psi$  values, the positive  $\Psi$  values are indicative of an antiestuarine cell. In Fig. 9 the results of such computation are shown. The model solution appears as a complex system of estuarine and antiestuarine cells varying in intensity, vertical and horizontal extension. The first cell (E1) is surface intensified and it is estuarine or wind driven, extending from the northern to the southern regions and is connected to river runoff and Ekman pumping in the surface layers. The second estuarine cell (E2) is positioned at the bottom of the Southern Adriatic, leaning toward the Otranto Strait sill. This bottom intensified estuarine cell is totally new and might be connected to deep waters not locally produced but

advected southward from the northern shelves of the basin.

In the southern Adriatic, two large anti-estuarine cells (A1 and A2) are present at mid-depth, one positioned on the Otranto Strait and the other on the northern part of the Southern Adriatic depression. The anti-estuarine cells are connected to the dense water formation processes occurring on the downward branch of the cells and then forcing the return flow with a slow interior upwelling motion. The only period with weak anti-estuarine circulation is winter 2001 (Fig. 9B) while the other two winters show intensification of the anti-estuarine cells. In 2001, the E1 and E2 cells almost connect, hinting to the fact that in this year the estuarine character of the circulation is enhanced, due to the large Po runoff of autumn 2000 and winter 2001 and the weaker winter cooling affecting the amount of deep waters formed, as discussed above. The estuarine cell is clearly due to the large WACC extension and strength during 2001 reinforcing the outflow and southerly mass exchange.

The interface depth between estuarine and antiestuarine cells varies strongly with the years and the seasons, going from 100 m in winter 2000 and 2002, to 400 m and deeper in the winter of 2001.

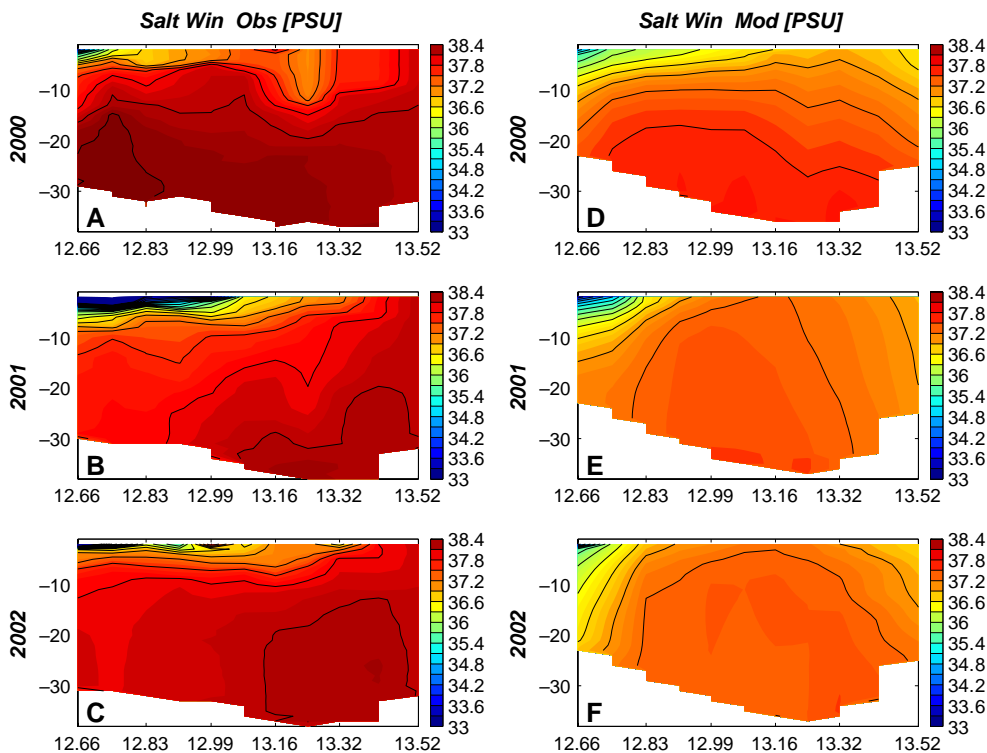


Fig. 11. Vertical salinity distributions (psu) along the transect A for the simulated winters. (A–C) 2000, 2001 and 2002 winters means from observations. (D–F) 2000, 2001 and 2002 winters means from model results.

### 3.3. Comparison between observations and model results

Observational activities in the Adriatic Sea for the period 2000–2002 include surveys of the northern Adriatic carried out within the MAT Project, and the NATO-SACLANT ADRIA-01 cruise. In order to assess the model performance, we have compared the model results with observations along two sampling transects of the MAT Project and with the basin-wide observations from the ADRIA-01 data survey.

The MAT data considered for this comparison have been collected along the transects A and C shown in Fig. 1 with an approximate monthly frequency (see Table 3 for a listing of the sampling dates). Samplings have been grouped by seasons and averaged. In order to carry out a consistent comparison with observations, model results corresponding to the MAT sampling dates have been similarly averaged. The observed and modeled winter temperatures distribution along the transect A are shown in Fig. 10. Observations for winter 2000 and 2002 (Fig. 10A and C, respectively) show a relatively well-mixed area in the easternmost part of the section and stratification in the western. Winter 2001 (Fig. 10B) appears quite different from

the years described above, as the whole section is warmer and with very weak stratification. This different structure is due to the averaging of unevenly sampled data since year 2001 is biased towards the winter conditions (cf. Table 3). The difference in values is instead due to the interannual variability. The model reproduces the observed interannual variability, as the modeled winter 2001 is warmer than that of the years 2000 and 2002. The agreement between spatial structures in the model and observations is less clear, as the model does not seem to reproduce the stratified structure in the western part of the section well, particularly in the years 2000 and 2002. For these years, the model seems to be affected by excessive mixing processes that do not maintain the observed stratification structure in the WACC region.

The observed and model-predicted salinity sections for the same season are shown in Fig. 11. In addition to the mixing problem pointed out above, the model-predicted salinity is lower than observed as a consequence of the missing inflow of very salty waters from the Ionian Sea and probably of an overestimation in the climatological river runoff from Adriatic rivers other than the Po. The differences between observed and climatological (Artegianni et al., 1997a,b) salinity for

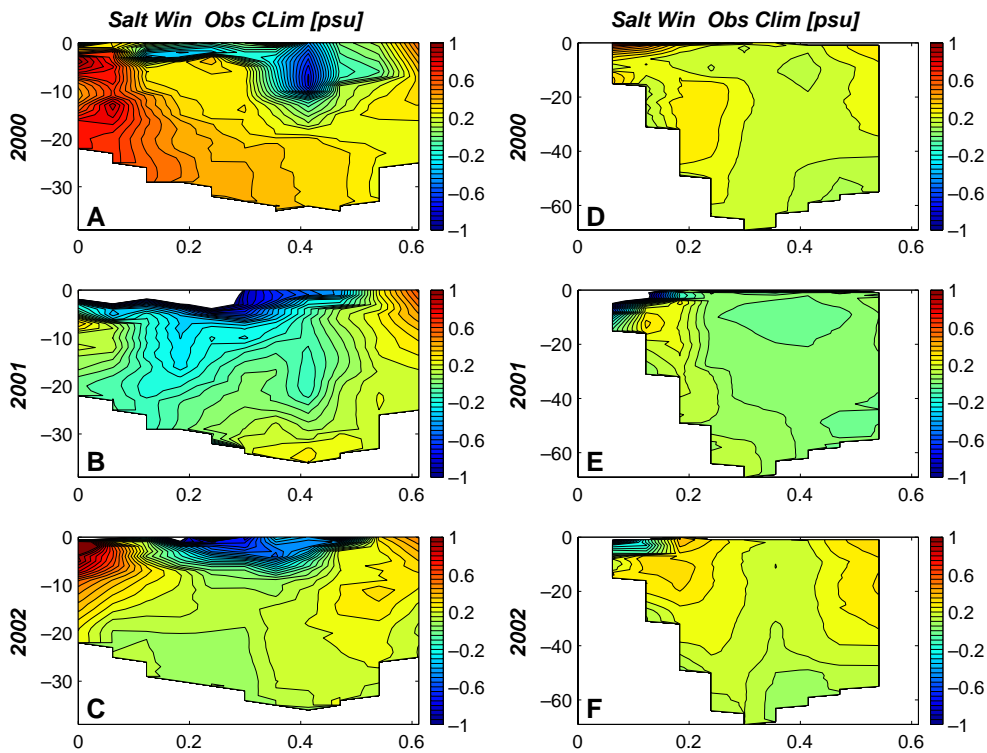


Fig. 12. Differences between climatological salinity (Artegianni et al., 1997a,b) and MAT project data along the transects A and C. (A) winter 2000, (B) winter 2001, (C) winter 2002, along transect A. (D) winter 2000, (E) winter 2001, (F) winter 2002, along transect C.

transects A and C during winter are shown in Fig. 12. The positive anomalies indicate that in 2000 and 2002, waters of higher salinity values than the climatology intruded in the Adriatic Sea and reached the northernmost part of the basin (transect A). We argue that this is the signal of the Aegean intermediate waters formed during the Eastern Mediterranean transient (Klein et al., 1999; Manca et al., 2002). Unfortunately, these waters are absent at the model open boundary in the Ionian Sea, thus giving rise to a large discrepancy between model solutions and observations.

The spring surface thermal gains determine the onset of a strong vertical stratification that is reproduced in a satisfactory way by the model along section C (Fig. 13). The observed and simulated temperatures are in the range between 22.5 °C near the surface and 11 °C on the bottom.

During the summer, along section C, (Fig. 14) the temperature and the stratification strengthen and a strong thermocline on the 20 m depth appears in the observations. The surface heat gain determines temperatures higher than 23 °C during all of the summers, with a minimum during 2001. The bottom cold waters are not influenced by the interannual variability of the seasonal warming and the temperature values are about

14 °C in all of the years. The model solution has a weaker stratification and seems to match the observed interannual variability characterized by a warmer 2002 summer well.

The two observed autumns of 2000 and 2001 (Fig. 15) along the section A are probably the seasons with the greatest signal of interannual variability. Modeled and observed autumns, along transect A of the year 2000, are characterized by high temperature and a stratification in the middle part of the section. In both the data sets, the signal of the WACC cold waters is evident. During 2001, the observed and simulated temperatures are quite different and the vertical processes seem to have an important role in the dynamics.

In order to gain a better insight of the model solution and its similarities with the observed data, we present a comparison between a horizontal field obtained from ADRIA01 (Fig. 16A) data set, covering the entire basin, and the model results (Fig. 16B). The ADRIA-01 data were collected during a period of about 20 days during February of 2001 and here they are considered synoptic and compared with the model predicted monthly mean for February 2001. The field of temperature at 5 m depth has been obtained applying an

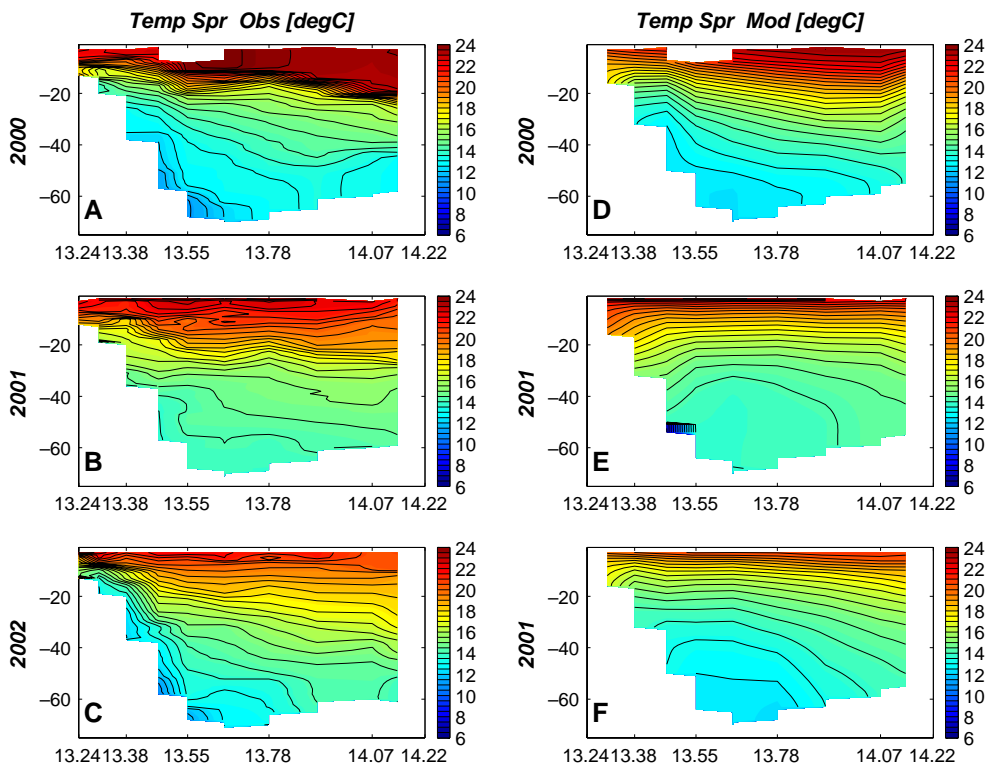


Fig. 13. Vertical temperature distributions (°C) along the transect C for the simulated springs. (A–C) 2000, 2001 and 2002 springs means from observations. (D–F) 2000, 2001 and 2002 springs means from model results. The position of the transect is reported in Fig. 1.

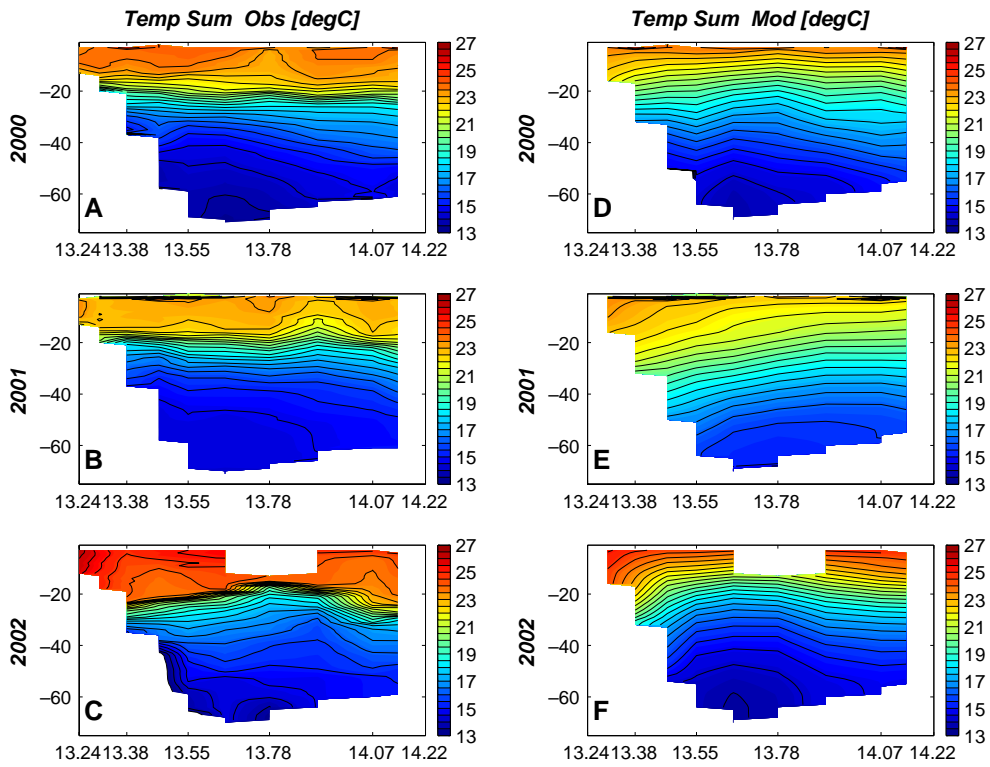


Fig. 14. Vertical temperature distributions (°C) along the transect C for the simulated summers. (A–C) 2000, 2001 and 2002 summers means from observations. (D–F) 2000, 2001 and 2002 summers means from model results.

objective analysis scheme (Carter and Robinson, 1987) to the ADRIA01 data set. The observed data shows a clear signal of the WACC and an inflow corresponding to the ESAC, carrying warm waters that reach the middle part of the basin. The simulated pattern of the WACC waters is wider and less intense than observed.

In the southern part of the basin, the model matches the west–east gradient found in the observed data. The difference between modeled and observed temperature around the latitude of 42°N (Gargano Peninsula) is probably related to the isotropic function used in the objective analysis.

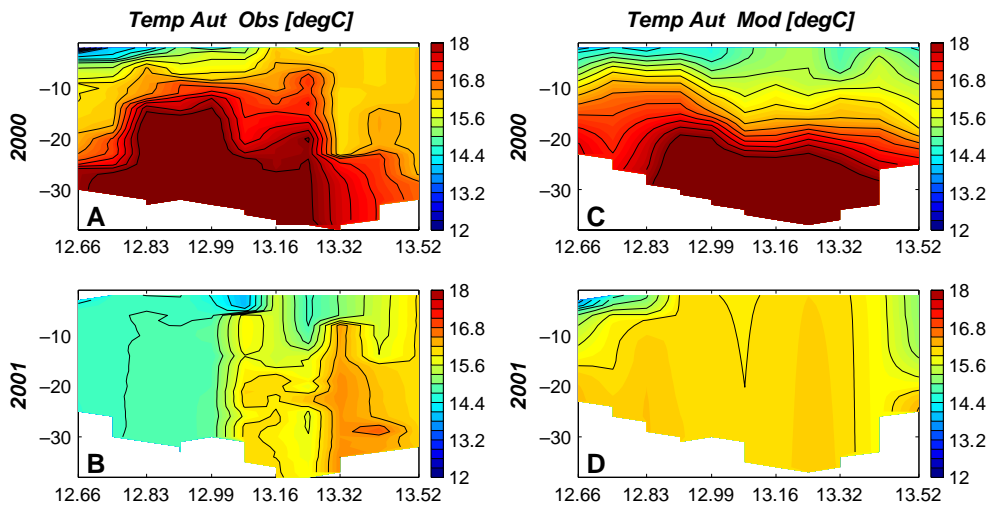


Fig. 15. Vertical temperature distributions (°C) along the transect A for the 2000 and 2001 autumns. (A–B) 2000 and 2001 autumns means from observations. (C–D) 2000 and 2001 autumns means from model results.

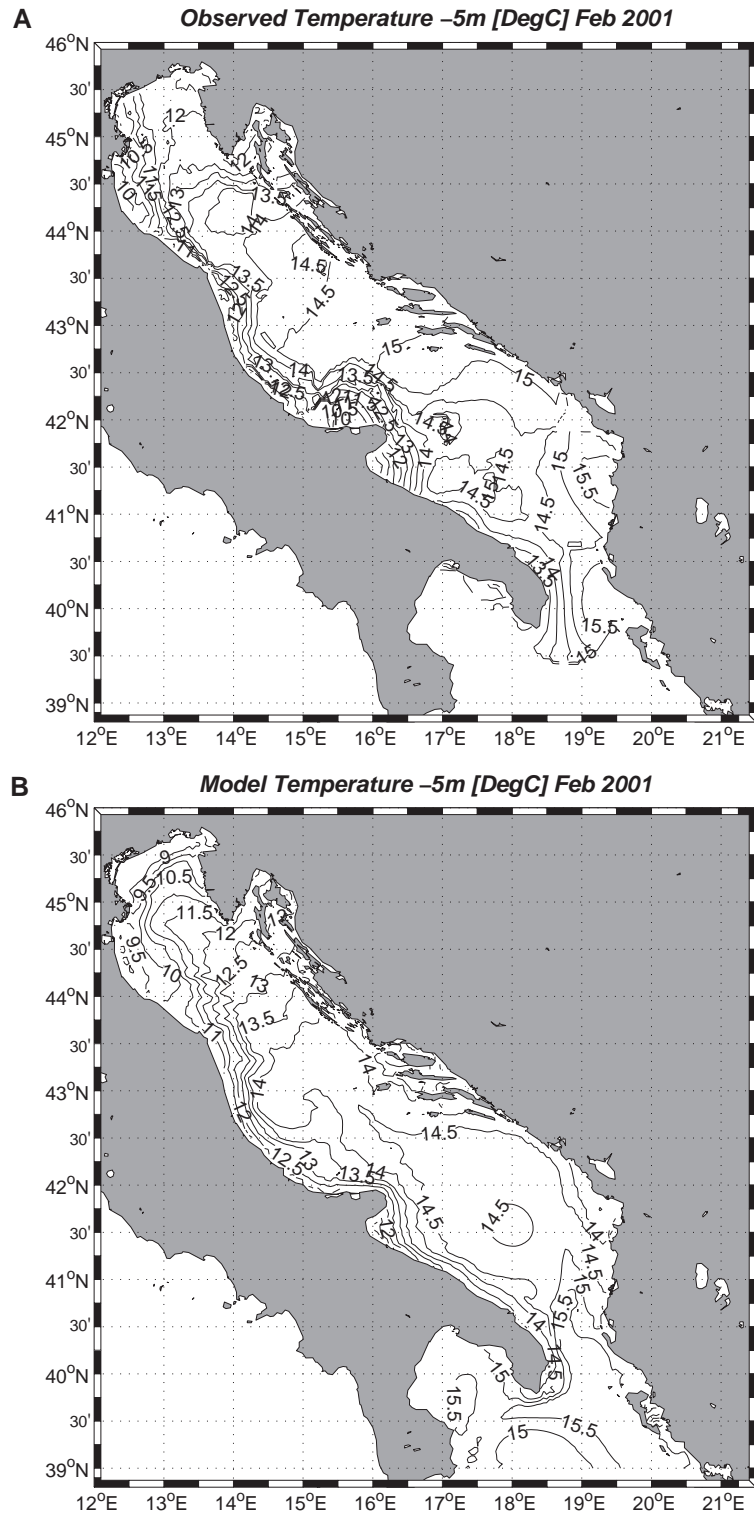


Fig. 16. February 2001 monthly mean near-surface (5 m depth) temperature ( $^{\circ}\text{C}$ ) from (A) ADRIA01 observations and (B) model results.

#### 4. Discussion and conclusions

This paper has described the 2000–2002 interannual variability of the Adriatic Sea circulation from model simulations. The model results show a strong interannual variability in intensity and characteristics of all the known physical circulation structures. The WACC is most intense in winter while in summer detaches the coast and forms meanders and anticyclonic eddies (Fig. 7). The NAd gyre is well reproduced and is particularly strong in summer. Its position and shape varies inter-annually and is characterized by the southernmost extension in summer 2002. The structure of the surface currents in summer 2001 is marked by the presence of the Istrian Coastal Countercurrent (Supic et al., 2000) even if, at this model resolution, the ICC is poorly resolved (Zavatarelli and Pinardi, 2003). The SAd gyre is well defined throughout the whole simulation period.

Overall, the years 2000 and 2002 are similar to each other, while 2001 is different mostly because of the characteristics of the autumn 2000 surface forcing and the winter–spring 2001 sustained freshwater Po runoff. The three sub-basins seem to be differently affected by the forcings functions. The dynamics of the northern and middle part of the basin are clearly the consequence of atmospheric forcing and the Po river runoff. The circulation in the southern part of the basin results from an equilibrium between atmospheric forcing and the inflow–outflow regime through the Otranto Strait. The most relevant atmospheric and river event observed during the studied period is the mild autumn–winter 2000–2001 with a large Po runoff producing no deep waters in the northern and middle Adriatic basins.

The basin thermohaline circulation has been diagnosed in terms of two estuarine and two anti-estuarine cells occupying different portions of the basin vertical and meridional extension. The surface is dominated by an estuarine cell that is very strong in 2001. The intermediate and deep waters in the southern Adriatic basin are dominated by two anti-estuarine cells connected to the local water formation mechanisms and inflow of LIW from Otranto.

The comparison with available observations shows a general overestimation in the vertical and horizontal mixing processes and a deficiency connected to the inflow of salty waters from the Ionian Sea. However, we noticed a good agreement between observed and simulated interannual trend. Future improvements involve the sensitivity to nesting boundary conditions, increase of the model resolution and data assimilation.

#### Acknowledgements

This work was partially funded by the Italian Ministry for the Environment and Territory (Adricosm project) through the University of Bologna, Centro Interdipartimentale per le Ricerche di Scienze Ambientali, Ravenna. We would like also to thank the MAT project and the NATO SACLANT Undersea Research Centre for making available data.

#### References

- Artegiani A, Azzolini R, Salusti E. On the dense water in the Adriatic Sea. *Oceanol Acta* 1989;12:151–60.
- Artegiani A, Bregant D, Paschini E, Pinardi N, Raicich F, Russo A. The Adriatic Sea general circulation Part I: air sea interaction and water mass structure. *J Phys Oceanogr* 1997a;27: 1492–514.
- Artegiani A, Bregant D, Paschini E, Pinardi N, Raicich F, Russo A. The Adriatic Sea general circulation Part II: baroclinic circulation structure. *J Phys Oceanogr* 1997b;27:1515–32.
- Blumberg AF, Mellor GL. A description of a three-dimensional coastal ocean circulation model. In: Heaps NS, editor. Three-dimensional coastal ocean models. Washington, DC: American Geophysical Union; 1987. 208 pp.
- Carter EF, Robinson AR. Analysis models for the estimation of oceanic fields. *J Atmos Ocean Technol* 1987;4:49–74.
- Castellari S, Pinardi N, Leaman K. A model study of air–sea interactions in the Mediterranean Sea. *J Mar Syst* 1998;18:89–114.
- Cardin V, Gacic M. Long Term heat flux variability and winter convection in the Adriatic Sea. *J Geophys Res* 2003;108:NO C9.
- Chiggiato J, Zavatarelli M, Deserti M, Castellari S. Comparison of Adriatic Sea surface fluxes estimated from different operational models data sets and local observations (1998–2001). *Sci Total Environ* this issue.
- Demirov E, Pinardi N. Simulation of the Mediterranean Sea circulation from 1979 to 1993: Part I The interannual variability. *J Mar Syst* 2002;33–34:23–50.
- Hellerman S, Rosenstein M. Normal monthly wind stress over the world ocean with error estimates. *J Phys Oceanogr* 1983;13: 1093–104.
- Jerlov NG. *Marine optics*. New York: Elsevier Sci.; 1976. 231 pp.
- Klein B, Roether W, Manca BB, Bregant D, Beitzel V, Kovacevic V, et al. The large deep water transient in the Eastern Mediterranean. *Deep-Sea Res* 1999;1.46:371–414.
- Kondo J. Air–sea bulk transfer coefficients in diabatic conditions. *Boundary-Layer Meteorol* 1975;9:91–112.
- Lascaratos A, Gacic M. Low-frequency sea level variability in the Northeastern Mediterranean. *J Phys Oceanogr* 1990;20:522–33.
- Legates DR, Wilmott CJ. Mean seasonal and spatial variability in a gauge corrected global precipitation. *Int J Climatol* 1990;10: 121–7.
- Maggiore A, Zavatarelli M, Angelucci MG, Pinardi N. Surface heat and water fluxes in the Adriatic Sea: seasonal and interannual variability. *Phys Chem Earth* 1998;23:561–7.
- Malanotte Rizzoli P. The northern Adriatic Sea as a prototype of convection and water mass formation on the continental shelf. In: Chu PC, Gascard JP, editors. *Deep convection and deep water formation in the Oceans* Elsevier Oceanography Series, vol. 57; 1991. p. 229–39.

- Manca BB, Kovacevic V, Gacic M, Viezzoli D. Dense water formation in the Southern Adriatic Sea and spreading into the Ionian Sea in the period 1997–1999. *J Mar Syst* 2002;33–34: 133–54.
- Marchesiello P, McWilliams JC, Shchepetkin A. Open boundary conditions for long term integration of regional oceanic models. *Ocean Model* 2001;3:1–20.
- May PW. A brief explanation of Mediterranean heat and momentum flux calculations NORDA Code 322. Stennis Space Center, Miss.: Nav Oceanogr Atmos Res Lab; 1986. 5 pp.
- Mellor GL. An equation of state for numerical models of ocean and estuaries. *J Atmos Ocean Technol* 1991;8:609–11.
- Mellor GL, Yamada T. Development of a turbulence closure submodel for geophysical fluid problems. *Rev Geophys Space Phys* 1982;20:851–75.
- Mellor GL, Blumberg AF. Modeling vertical and horizontal diffusivities with the sigma coordinate ocean models. *Mon Weather Rev* 1985;113:1379–83.
- Orlic M, Gacic M, La Violette P. The currents and circulation of the Adriatic Sea. *Oceanol Acta* 1992;15:109–24.
- Orlic M, Kuzmic M, Pasaric Z. Response of the Adriatic Sea to the Bora and Sirocco forcing. *Cont Shelf Res* 1994;14:91–116.
- Ovchinnikov IM, Zats VI, Krivoskeya VG, Nemirovsky MS, Udodov AI. Winter convection in the Adriatic and formation of deep eastern Mediterranean waters. *Ann Geophys* 1997;5B:89–92.
- Peixoto JP, Oort AH. *Physics of climate*. American Institute of Physics; 1992. 520 pp.
- Pinardi N, Allen I, Demirov E, De Mey P, Korres G, Lascaratos A, et al. The Mediterranean ocean forecasting system: first phase of implementation (1998–2001). *Ann Geophys* 2003;21:3–20.
- Poulain MP. Adriatic Sea surface circulation as derived from drifter data between 1990 and 1999. *J Mar Syst* 2001;29:3–32.
- Provini A, Crosa G, Marchetti R. Nutrient export from the Po and Adige river basin over the last 20 years. *Sci Total Environ* 1992;291–313 [suppl.].
- Raicich F. Note on flow rates of the Adriatic rivers, Istituto Talassografico Sperimentale Trieste. Technical Report; 1994;RF02:94, 8.
- Raicich F. On fresh water balance of the Adriatic Sea. *J Mar Syst* 1996;9:305–19.
- Reed RK. An evaluation of formulas for estimating clear sky insolation over the ocean. NOAA-ERL 352-PMEL Technical Report 1975;26:25.
- Reed RK. On estimating insolation over the ocean. *J Phys Oceanogr* 1977;1:854–71.
- Sannino GTM, Bargagli A, Artale V. Numerical modelling of the mean exchange through the Strait of Gibraltar. *J Geophys Res* 2002;107(C8). doi:10.1029/2001JC000929.
- Smagorinsky J. Some historical remarks on the use of nonlinear viscosities. In: Galperin B, Orszag SA, editors. *Large eddy simulations of complex engineering and geophysical flows*. New York: Cambridge Univ. Press; 1993. p. 3–36.
- Smolarkiewicz PK. A fully multidimensional positive definite advection transport algorithm with small implicit diffusion. *J Comput Phys* 1984;54:325–62.
- Supic N, Orlic M, Degobbi D. Istrian coastal countercurrent and its year-to-year variability. *Estuar Coast Shelf Sci* 2000;51: 385–97.
- Vilibic L. An analysis of dense water production on the North Adriatic shelf. *Estuar Coast Shelf Sci* 2003;56:697–707.
- Zavatarelli M, Pinardi N, Kourafalou VH, Maggiore A. Diagnostic and prognostic model studies of the Adriatic Sea circulation Seasonal variability. *J Geophys Res* 2002;107(C1) [art 3004].
- Zavatarelli M, Pinardi N. The Adriatic Sea modelling system: a nested approach. *Ann Geophys* 2003;21:345–64.